

Measuring Polarization Rotation to study Spin-exchange Collisions

Jeffrey S. Eldred *REU program, College of William and Mary*
I. B. Novikova *College of William and Mary, Physics Dept.*

August 14, 2009

Abstract

Spin-exchange collisions is a well established means of preserving spin-coherence by the transferring the spin state of highly polarizable atoms with a high coherence decay to atoms with lower coherence decay rates. This paper attempts an experimental measure of spin-exchange collisions for a superposition of spin-states caused by the Zeeman effect. The polarization rotation caused by the nonlinear Faraday Effect as a laser interacts with the atomic Rubidium (Rb) vapor allows one to infer the coherence of the superposition of spin-states generated by the laser. If the presence of the control laser tuned to a transition in the ^{85}Rb vapor is able to affect the polarization rotation of the probe laser tuned to a transition in ^{87}Rb , than this would indicate that the quantum state in one atom was preserved in the paraffin coated cell and was able to transfer that quantum state to another atom. If this effect is present in our experiment, it is difficult to verify because it has a low impact on the polarization rotation relative to noise. It is necessary to take more data in order to confirm the spin-exchange collisions effects and as a prerequisite for studying the dynamics of this system.

Supported by NSF REU grant PHY-0758010

1 Introduction

It is already quite clear that atoms in vapor prepared with electrons in a certain spin state can transfer that spin coherence to other atoms in that vapor via a process known as spin-exchange collisions. This is a well-established technique in physics that has been successfully been used in diverse application from particle accelerator targets to medical imaging. What is less clear is whether or not a superposition of spin-states can be effectively transferred this way, as would be necessary for some quantum information storage applications. Currently, the highly polarizable alkali metals suffer from the drawback of having a short coherence lifetime which is undesirable for storing quantum information. If spin-exchange collisions can transfer this state to a more stable atom, quantum information stored this way would be able to remain coherent for much longer periods of time.

2 Spin-Exchange Collision Effects

When a laser is tuned to an atomic transition of a Rb isotope in the presence of a magnetic field, the atom is put into a superposition of spin states, and the polarization of the laser light is rotated proportionately. One can tune one laser to a transition in ^{85}Rb and tune a non-overlapping laser

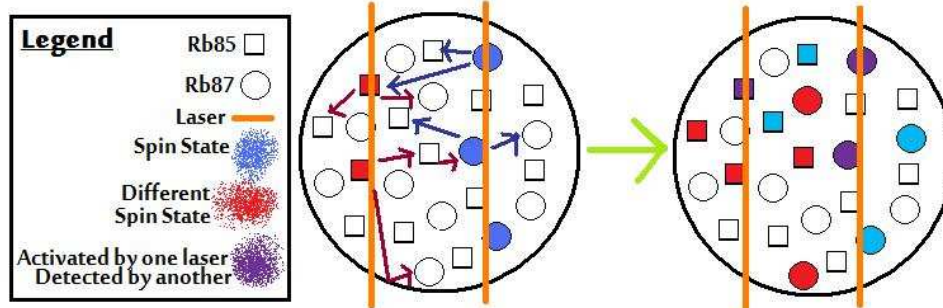


Figure 1: If a laser interacting with one isotope can change the interaction of the second laser with a second isotope, than this can only have occurred through a spin-exchange collision

to a transition in ^{87}Rb and test whether one laser can have an effect on the polarization rotation of the other. That effect would indicate that the first laser (the control laser) prepared one isotope of Rb with a spin state, that the atom kept that state while it bounced off the paraffin coated walls, transferred it to the other isotope via spin-exchange collisions, and caused a rotation in the polarization of the second laser (the probe laser). See Figure 1 for a rough sketch of the concept.

3 Nonlinear Faraday Rotation

Figure 2 displays the valence level structure of ^{87}Rb with the Zeeman splitting from a magnetic field [1]. The ^{85}Rb structure is identical, except with different frequencies corresponding to the atomic energy levels. If the frequency of a laser is tuned so that its energy level matches the atomic transition of a hyperfine state, then the electron oscillates at the Rabi frequency between the corresponding excited $5s_{1/2}$ hyperfine state and the $5p$ state. When the $5p$ electron state decays to the $5s_{1/2}$ hyperfine state that resonant with the laser frequency, the electrons simply becomes excited again. When the $5p$ electron state decays to the $5s_{1/2}$ hyperfine state that is off-resonant, than the electrons remain in the state comparatively longer. This is known as optical pumping and the result is a deficit of electrons in the resonant hyperfine state and surplus of the electrons in the off-resonance hyperfine state.

In the influence of a magnetic field, the hyperfine energy levels split into Zeeman sublevels and the optical pumping leaves the electrons in a superposition of Zeeman sublevels that is not uniform. In addition, the finite amount of time it takes for an excited $5p$ state to decay down to the $5s_{1/2}$ states creates a relative phase shift from the period of the Rabi cycle. This process generates the phase shift in the polarization of light as it propagates through the Rb vapor cell. While the accurate mathematical description of this is beyond the scope of this undergraduate research project, a full representation of the density matrix formulation of this system can be found in Joe Goldfrank's thesis [2]. The dynamics of the system are described in qualitative terms of known forces in a paper by Budker, Yashchuk, and Zolotarev [3]. Laser light tuned to the atomic transitions in Rb propagates through the laser cell with a certain polarization orthogonal to the direction of propagation of the laser light. The Rb atoms align their magnetic moment in the direction of the polarization. In the presence of an applied longitudinal magnetic field, Larmor precession takes place and the magnetic moment of the atom rotates about that longitudinal axis.

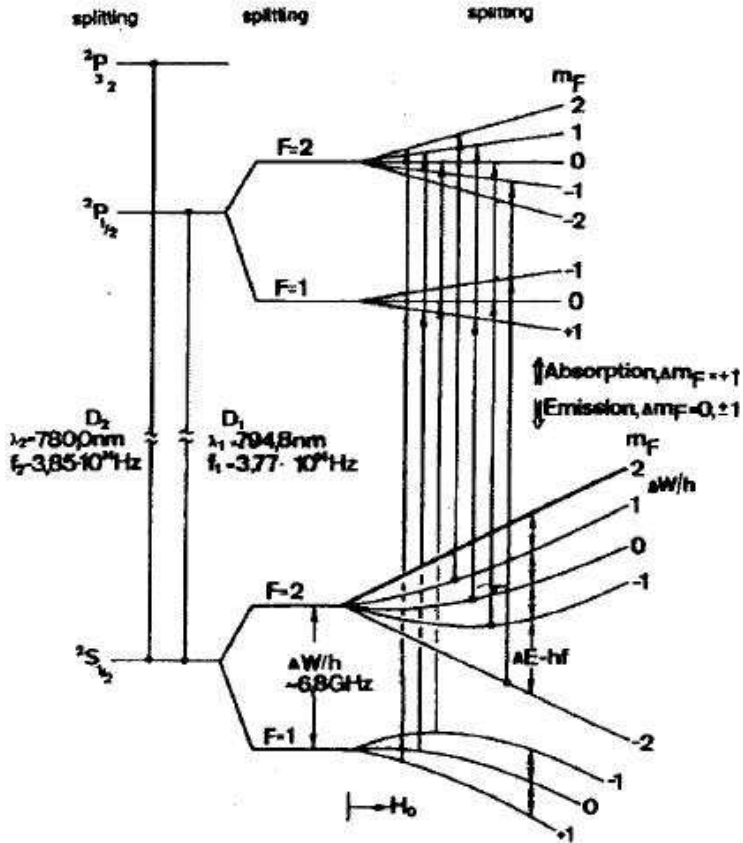


Figure 2: Energy level diagram of ^{87}Rb with hyperfine splitting and Zeeman splitting [1]

There is a net magnetization in the vapor-cell which and as an electromagnetic wave, light is modified by it. Faraday rotation takes place and the laser receives a net rotation in polarization towards that of the sample. In reality, Faraday rotation and Larmor precession do not take place as discrete processes as this description implies, but rather the magnet field orthogonal to the polarization of the light uses quantum state of the Rb vapor as a medium to have a rotational effect on the polarization of light and this process occurs in time only as the laser light activates the Rb.

4 Experimental Setup

The experimental setup used is shown in Figure 4. There are two lasers of tunable frequency, the first one is able to cover the spectrum in which the D1 transitions occur in each of the ^{85}Rb and ^{87}Rb isotopes and the other for those of the D2 transitions (see Figure 2). The lasers are aligned parallel but with non-overlapping beam spots. The control laser passes through a $\lambda/2$ waveplate and both lasers pass through a polarizer so that the polarization incident to the Rb test cell is the same in both lasers and so the control laser can be attenuated independently of the probe laser. A small portion of both lasers is directed to a “reference” Rb cell and the rest is raised by a periscope

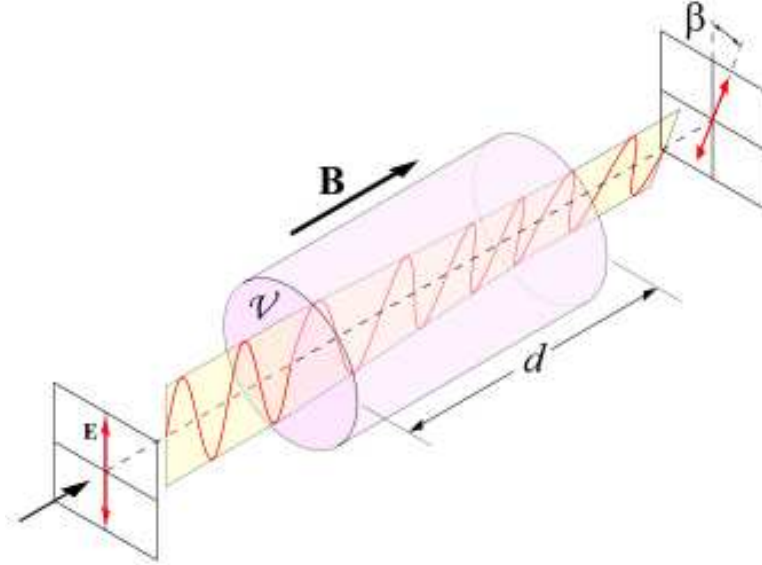


Figure 3:

and directed through the “test” Rb cell. In the reference Rb cell, the laser light passes through the cell, is attenuated by a filter, passes back through the cell and is focused onto a photodiode. The signal on the photodiode as a function of frequency is characterized by a wide decrease in transmission around atomic resonances due to Doppler broadening and a smaller, sharper peak at each resonance due to saturated absorption. This reference signal makes it possible to readily identify the atomic transitions that the laser activates as it sweeps through the spectrum.

The test Rb cell is surrounded by two pairs of Helmholtz coils (one set transverse and the other set longitudinal) controlled by a current source. These coils are surrounded by three layers of mu-metal for electromagnetic shielding and there are poles for degaussing the shielding. Like the reference Rb cell, the test Rb cell is heated to a desirable vapor pressure, but is also equipped with thermistors for recording the temperature. To ensure that any Rb condensation on the cell windows does not interfere with the transmission of the laser light, the Rb test cell has a tip that is distanced from the portion that makes the cylindrical laser target and is kept about four degrees cooler via a small air pressure ventilation system. There are pinholes on either side of the Rb test cell that can be used to block on laser or the other, before or after interacting with the Rb test cell.

During testing the Rb test cell is kept hot (56 to 58 degrees C) with the condensation confined to the tip and the temperature of both the main cell and the tip is measured before taking data. The electromagnetic shielding is degaussed to remove any irregular magnetic domains formed by warping of the mu metal in handling. A current source is turned on and is set manually to deliver a constant current of 135 mA to the longitudinal Helmholtz coils. According to tests performed by J. Goldfrank [2], 135mA corresponds to a constant magnetic field of 593 mG.

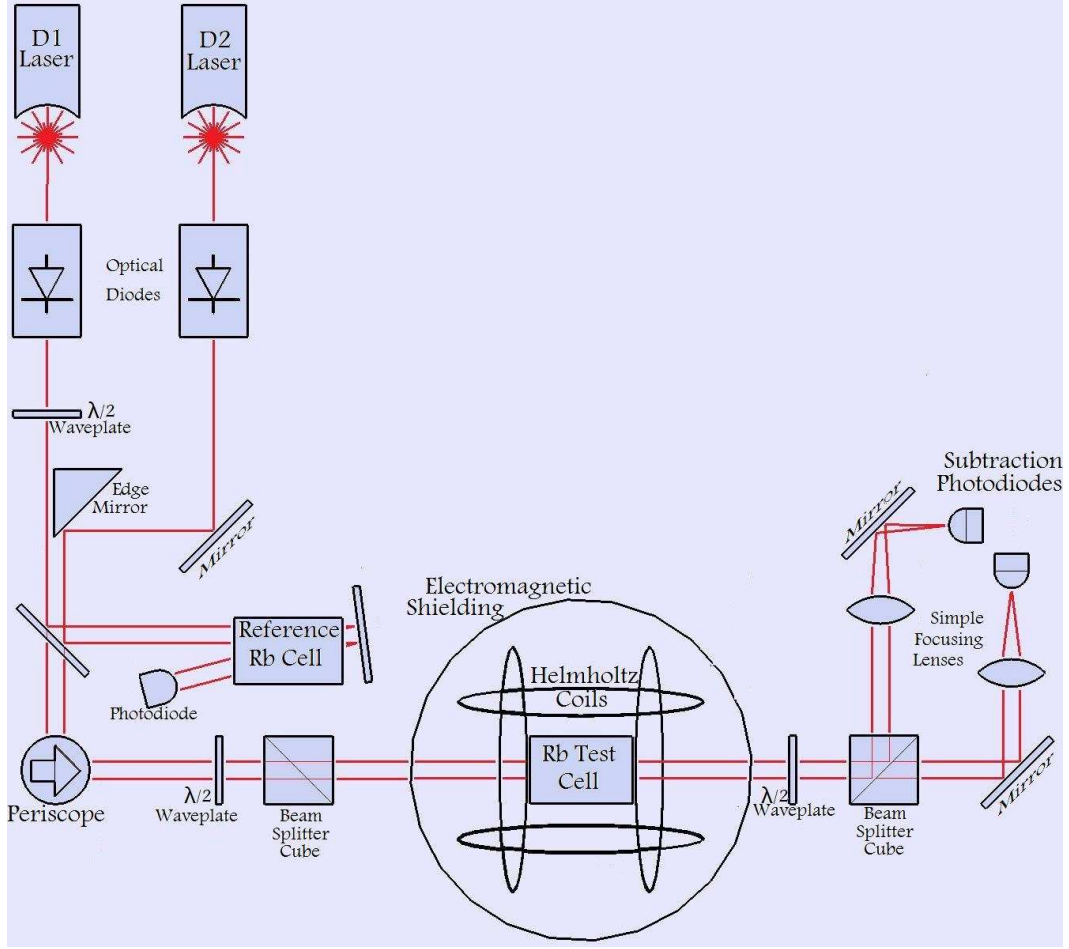


Figure 4: First the lasers are aligned parallel to each other, then a reference signal is split off for saturated absorption spectroscopy and the rest are directed through the test cell and the polarization rotation is measured.

5 Polarization Rotation Measurements

After the Rb test cell the lasers are passed through a system designed to measure the difference in polarization between light tuned to an atomic transitions of Rb and off resonance frequencies (with the incident polarization). The lasers hit a beam-splitter cube which transmits or reflects light based on its polarization and directs the light traveling in each channel to be focused onto a photodiode for measurement. The intensity in each channel is given by Equation 1 and Equation 2, and the solution in terms of θ is given in Equation 3.

$$I_1 = \frac{1}{2}I + \frac{1}{2}I\sin(2\theta) \quad (1)$$

$$I_1 = \frac{1}{2}I - \frac{1}{2}I\sin(2\theta) \quad (2)$$

$$\theta = \frac{1}{2} \arcsin \left(\frac{I_1 - I_2}{I_1 + I_2} \right) \quad (3)$$

Figure 5 graphs the intensity in each channel as a function of θ . There is a waveplate in the setup

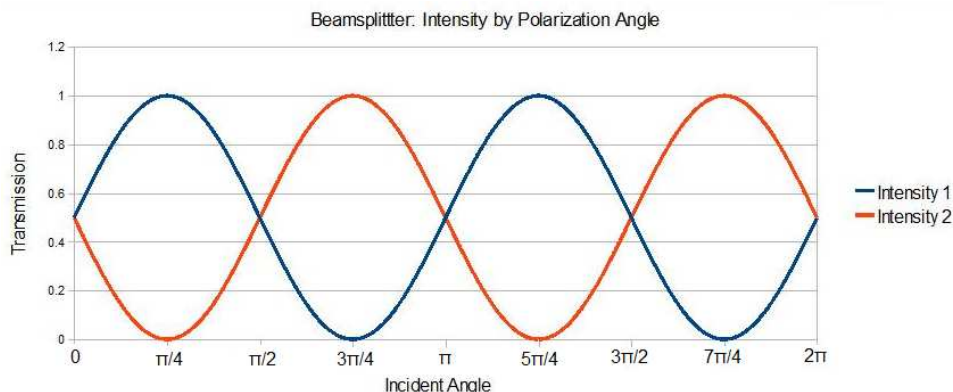


Figure 5: The total light remains the same but the light in any given channel varies from all to nothing depending on θ

that allows one to pick the polarization angle of light to the beamsplitter relative to that of light entering the Rb test cell. To achieve the maximum sensitivity of light intensity to changes in θ , we take our measurements in the regime where the absolute value of the derivative of the intensity in each channel is maximized - when the intensity in each channel is matched. Here, a small angle approximation of Equation 3 is appropriate and the polarization rotation is linearly proportional to the difference in intensity. To minimize noise due to instability of the gain used to amplify electronic circuits, the photodiodes are connected to a differential amplifier that automatically takes the difference of the two signals. We can directly use this signal as an indicator of rotation of the polarization of the incident laser light due to the quantum state of the Rb atoms. The primary means of testing the hypothesis is to identify the extent to which a possible spin-exchange collision effect deviates from background noise, so the measurements are significant only in relation to each other and the units of data presented are arbitrary.

To investigate the stability of the lasers and the beamline elements, one simply observes the deviation in time about $I_1 - I_2 = 0$ over time. While there was no quantitative data taken, this technique indicated that the beamline stability was not as high as we would like it to be. The periscope which raises the beamline from the reference cell height to the test cell height was previously made out of two independent mirrors and fixed to adjustable height optical mounts. By replacing this with a single post to which both mirrors were affixed generated a significant improvement in stability.

6 Measurements

The measurements were taken for the lasers tuned to each of two different combinations of atomic transitions. The first combination of atomic transitions was chosen because it had originally appeared to have a strong effect and now serves as a comparison of how no effect appears. The first

combination of atomic transitions was the D1 laser as the probe laser tuned to ^{87}Rb $F=2 \rightarrow F'=1$ transition and the D2 laser as the control laser tuned to ^{85}Rb $F=3 \rightarrow F'=4$ transition. The second combination of atomic transitions was chosen because it is more directly applicable to quantum information storage. The second combination of laser transitions was the D1 laser as the probe laser tuned to ^{87}Rb $F=1 \rightarrow F'=1$ transition and the D2 laser as the control laser tuned to the ^{85}Rb $F=2 \rightarrow F'=1$ transition. For both combinations of atomic transition studied there are two types of measurements are taken. For the first the probe laser sweeps through the full range of frequencies in the presence of a constant magnetic field and for the second the probe laser is fixed to the frequency of the desired atomic transition and the magnetic field is swept.

Whether the measurements are taken with a sweeping laser frequency or a sweeping magnetic field, the procedure for taking the data is the same. The control laser is blocked after it interacts with the Rb test cell, so the polarization rotation that is measured comes solely from the probe laser. The light from the probe laser when there is no control laser (the control laser is blocked before it interacts with the Rb test cell) is compared to the light from the probe laser when selected intensities of the control laser interact with the Rb test cell. There appears to be some drifting in the laser that has a dependence on time, and therefore data must be taken in a way so that time is not a confounding variable. This is done between alternating between data-sets with no control laser light and measurements with selected intensities of the control laser. In this way the measurements with no control laser light can be averaged to represent how the data would look at the time the measurement with the control laser is taken. With each measurement that includes the control laser, the intensity is changed. Over the course of the measurements, data is taken as the control laser rises from minimum intensity to maximum intensity, back down to minimum, and back up to the maximum intensity.

Before taking data, it is necessary to setup up the experiment and verify that the independent variables and controls actually have the settings that the data would report. To start, the light from both lasers are attenuated so that no photodiode is saturated. The D1 laser is blocked and the D2 control laser is fixed to the desired atomic transition (which is identified by using the reference signal). Then the light from the D2 control laser is blocked instead of D1 and the probe laser is set to sweep through the full range of D1 ^{85}Rb and ^{87}Rb frequencies with no mode hops. The final $\lambda/2$ waveplate is adjusted so the signal in the subtraction photodiodes when D1 is sweeping over off-resonance frequencies is zero. The intensity of light from the probe laser and at various attenuations of the control laser is measured. The laser light from the control laser is blocked after the Rb test cell by the pinhole and it is verified that no significant signal is recorded when the probe laser is also blocked.

The first type of measurements is taken, with the probe laser sweeping and the magnetic field held constant. For the second type of measurements, the probe laser is fixed to the desired frequency. The current source to the Helmholtz coils is set to receive the analog signal from the function generator, which corresponds to a 700 mHz triangle wave alternating between -352 mG and 435 mG. The whole procedure repeated for the lasers tuned to the other combination of atomic transitions in Rb.

7 Data and Analysis

The graph of polarization rotation as the probe laser sweeps and the control laser is fixed to the ^{85}Rb $F=2 \rightarrow F'=1$ transition at various intensities is presented in Figure 6. The black curve on the

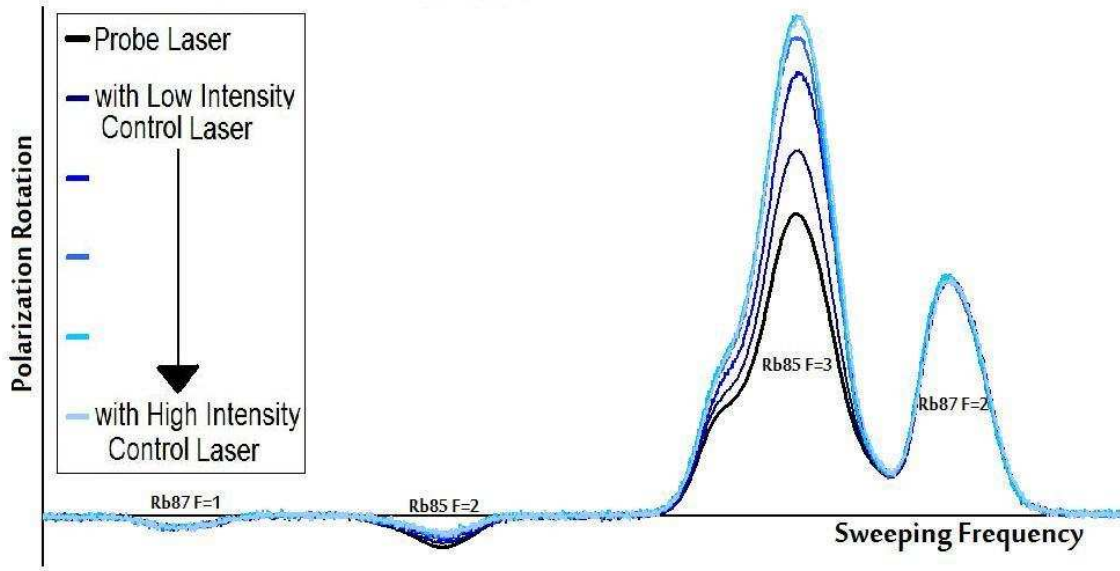


Figure 6: The polarization rotation is observed as the probe laser sweeps in the presence of a fixed magnetic field and at different intensities of the control laser which is fixed to the ^{85}Rb $F=2 \rightarrow F'=1$ transition

graph is the average of all the data-sets with the probe laser and no control laser. The remaining curves are average from the data-set at various intensities of the control laser and are indicated by a lighter blue as the intensity increases. For convenience, the constant offset of all the curves on the graph was adjusted so that the off-resonance portions of the curves equal. We see a clear trend of an increasingly dramatic departure from the probe field at ^{85}Rb resonances as with increases in the intensity of the ^{85}Rb tuned laser. This indicates that the optical pumping in ^{85}Rb is caused by the control laser, that these states remained coherent as they passed into the beam path of the probe laser, and that this had a rotation effect on the polarization of the probe laser at resonance distinct from the rotation effect on off-resonance portions. To make this rotation effect clearer, Figure 7 presents the same graph, except with the curve of the probe laser subtracted off of the others. To be specific, data-sets with no control laser are averaged with the next data-set with no control laser and subtracted from the data-set in between them, in which the control laser interacts with the Rb test cell. These modified data-sets are averaged by intensity and graphed in Figure 7. There appears to be some noise with no clear relation to the intensity of the control field as the laser sweeps across ^{87}Rb $F=2$ transition. This noise is of opposite sign on each side of the Rb 87 $F=2$ transition where the probe laser has a sharp peak and this occurs because drifting in the frequency of the probe laser generates noise that is to be sensitive to high slopes. There does not appear to be any discernible effect on the ^{87}Rb $F=1$ transition, as the probe field sweeps. Figure 8 presents the graph as the probe laser is fixed to the ^{87}Rb $F=1 \rightarrow F'=1$ transition and the magnetic field sweeps. Figure 9 represents figure 8 with the curve of the probe laser subtracted off, the color coding indicates the same things as Figure 6 and 7, and the data is averaged in the same way as Figure 6 and 7. Figure 9 seems to have a small correlation between rotation effect and magnetic field in a manner proportional to the intensity of light that deviates from noise. This is

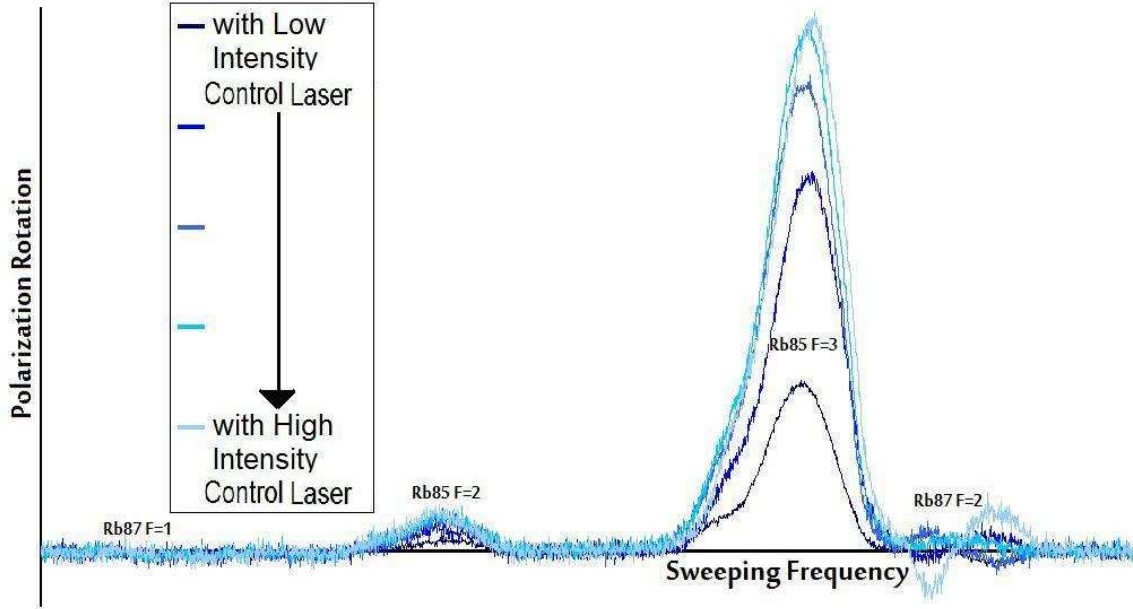


Figure 7: The deviation in polarization rotation between the probe laser with no control laser and the probe laser in the presence of a control laser interacting with the Rb test cell - as a function of probe laser frequency

a weak effect however - The signal to noise ratio is smaller than would be preferred and the lack of a trend in the ^{87}Rb F=1 in Figure 7 runs contrary to this data. It is useful however, to compare all of this to data in which the lasers are tuned to a different combination of transitions and it is much clearer that no spin-exchange collision effect has occurred. Figure 10 and Figure 11 are prepared and graphed in the same manner as Figure 6 and Figure 7 respectively, but is taken with the control laser tuned to the ^{85}Rb F=3 \rightarrow F'=4 transition instead. In Figure 10 optical pumping by the control laser has similar polarization rotation effects as in Figure 6 and in Figure 11 we see a similar pattern of the ^{87}Rb F=2 transition engulfed in noise and the ^{87}Rb F=1 wholly unresponsive to changes in control laser intensity. As before, Figure 12 and Figure 12 are a direct parallel to Figure 8 and Figure 9, respectively, except with the probe laser fixed to ^{87}Rb F=2 \rightarrow F'=1 transition instead. In Figure 13 however, the intensity of the control lasers shown no trend since they are all overlapping except the middle intensity, which slopes in the opposite direction. While the data is clearly nonzero, the noise is too great to conclude that there is any polarization rotation effect occurring due to spin-exchange collisions. This demonstrates that the data presented in Figure 9 needs further verification.

8 Conclusion

The correct operation of the experimental setup was confirmed by measurements of improved beam stability over time, of polarization rotation about resonance frequencies tuned to the atomic transitions of Rb, and of the effect of optical pumping from the control laser on the rotation of

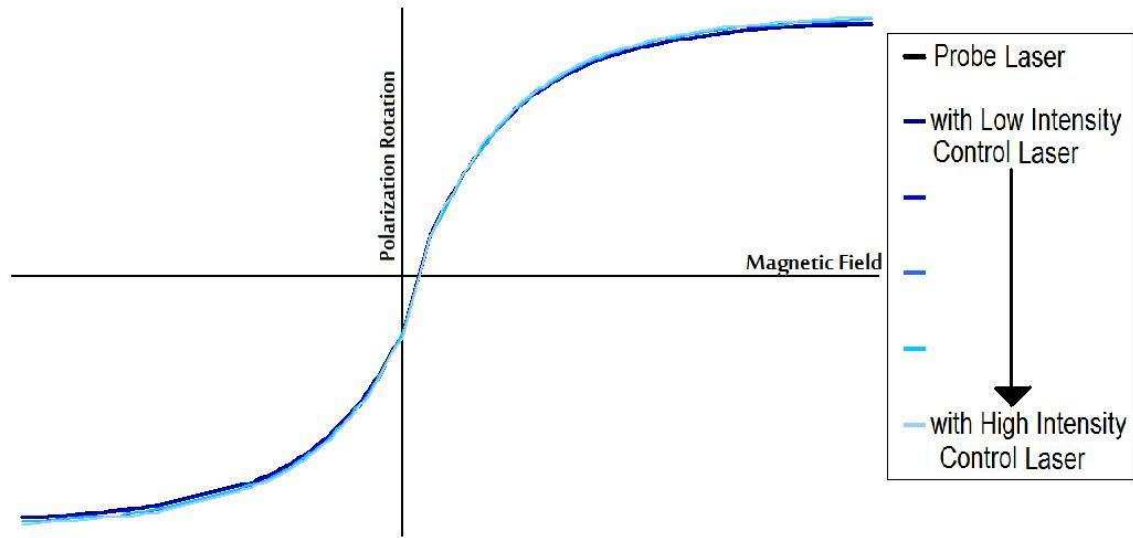


Figure 8: The polarization rotation is observed as the magnetic field sweeps with the control laser is fixed to the ^{85}Rb $F=2 \rightarrow F'=1$ transition and the probe laser fixed to the ^{87}Rb $F=1 \rightarrow F'=1$ transition

probe laser tuned to the same isotope.

Further examination is needed to make any reliable conclusion about whether or not this experiment has observed spin-exchange collision effects. If Figure 9 is demonstrated a spin-exchange collision effect, than it is difficult to be sure that it is not just a result of the noise or control light leaking through the pinhole in an unaccounted for manner.

If spin-exchange collision effects can be confirmed than the next step would be to study the dynamics of the system. Such an experiment would take rapid (or precisely timed) measurements of the effect of adding the light from the control laser to that of the probe laser over time. This process starts from the point in time at which the control laser is applied to the point in time at which the atomic state reaches a new equilibrium (similar to the data presented in this paper).

9 Acknowledgments

I would like to thank Professor Irina Novikova for allowing me the opportunity to work in her lab and guiding me through my research project. I am grateful for Joe Goldfrank's prior work on the experimental apparatus that I have built upon. This is made possible by Professor WJ Kossler, the William & Mary REU program, and National Science Foundation (NSF) funding through Grant number PHYS-0758010.

References

- [1] J. Recht and W. Klein. Optical pumping of rubidium. Technical report, U. Wisconsin, 2005.

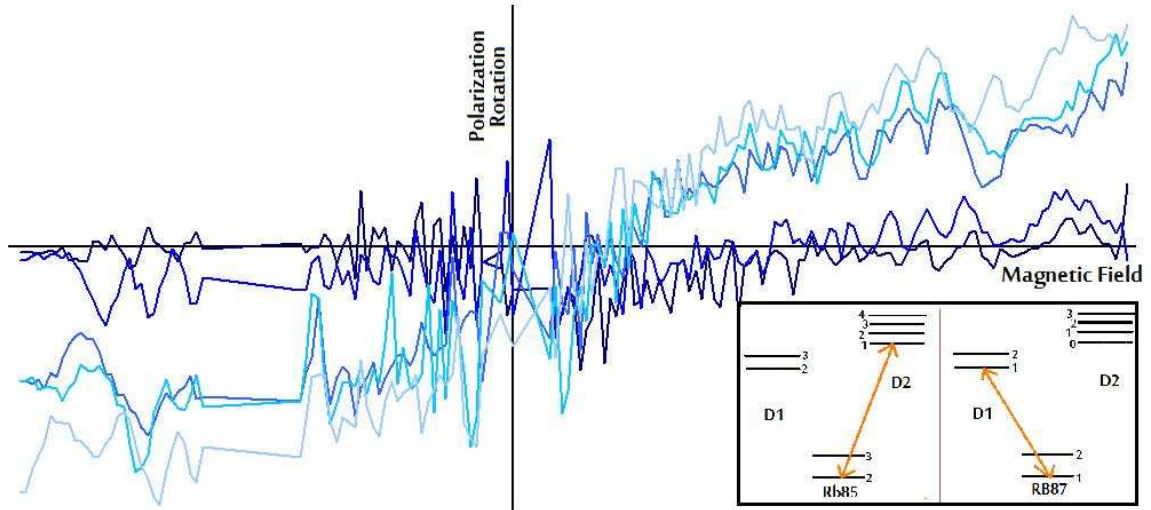


Figure 9: The deviation in polarization rotation between the probe laser with no control laser and the probe laser in the presence of a control laser interacting with the Rb test cell - as a function of magnetic field

- [2] J. Goldfrank. Collisional transfer of atomic coherence, 2009. B.S. Thesis, College of William and Mary.
- [3] Dmitry Budker, Valeriy Yashchuk, and Max Zolotarev. Nonlinear magneto-optic effect with ultranarrow widths. *Phys. Rev. Lett.*, 81:5788, 1998.

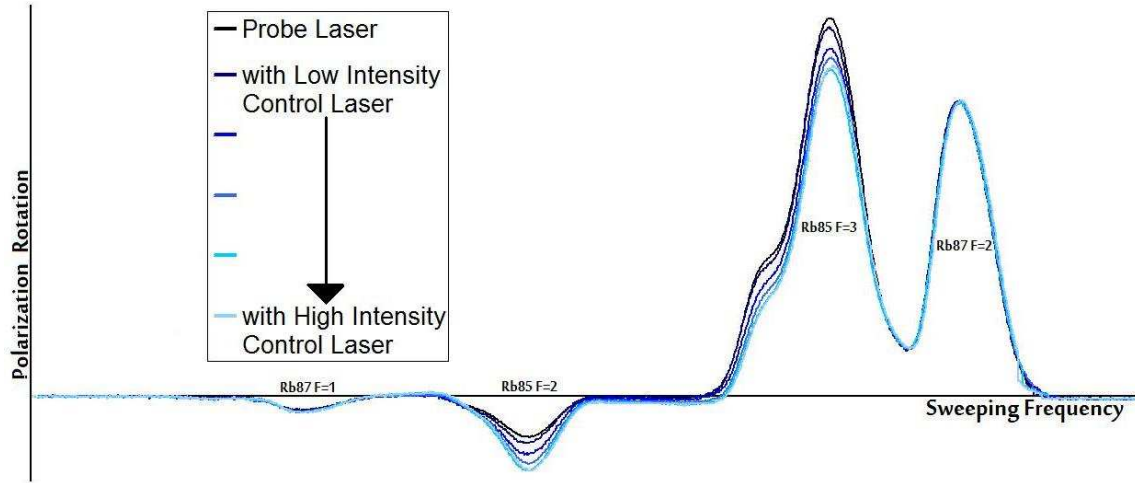


Figure 10: The polarization rotation is observed as the probe laser sweeps in the presence of a fixed magnetic field and at different intensities of the control laser which is fixed to the $^{85}\text{Rb } F=3 \rightarrow F'=4$ transition

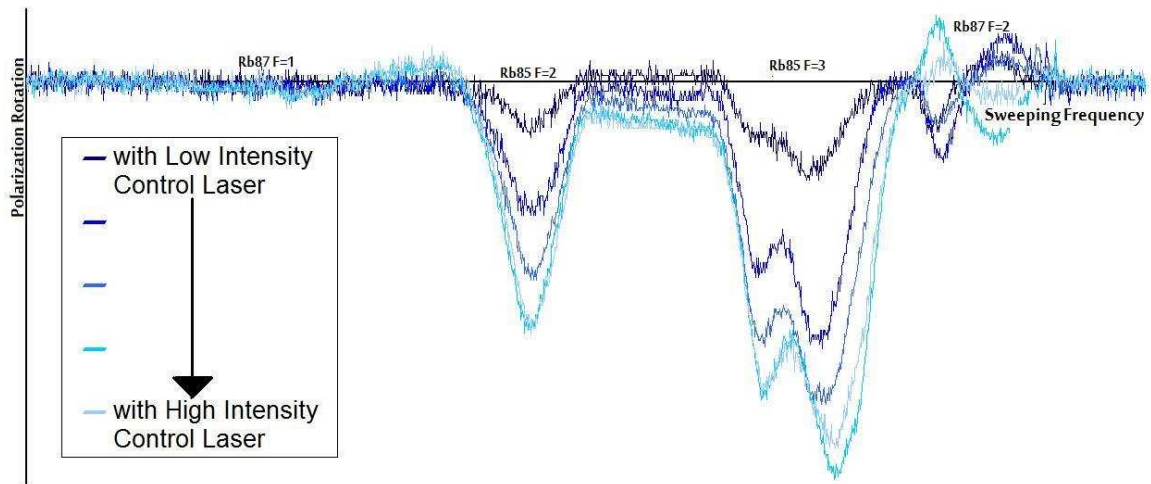


Figure 11: The deviation in polarization rotation between the probe laser with no control laser and the probe laser in the presence of a control laser interacting with the Rb test cell - as a function of probe laser frequency

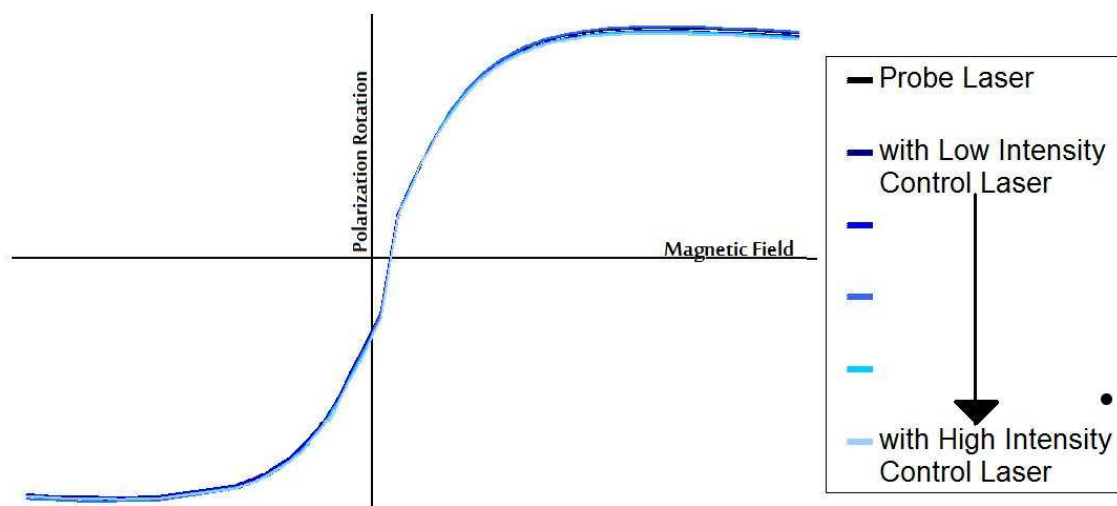


Figure 12: The polarization rotation is observed as the magnetic field sweeps with the control laser is fixed to the ^{85}Rb $F=3 \rightarrow F'=4$ transition and the probe laser fixed to the ^{87}Rb $F=2 \rightarrow F'=1$ transition

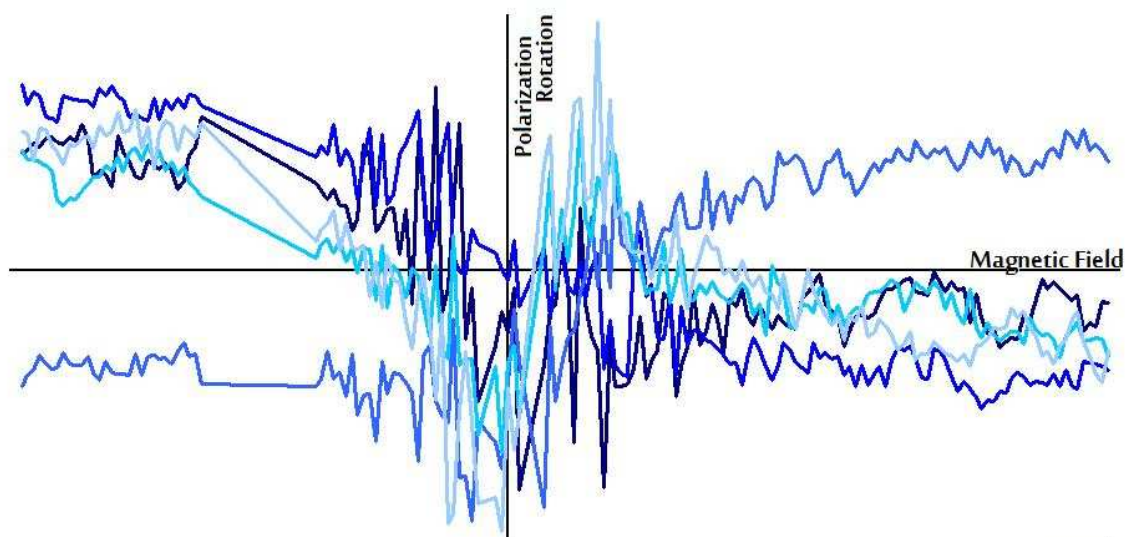


Figure 13: The deviation in polarization rotation between the probe laser with no control laser and the probe laser in the presence of a control laser interacting with the Rb test cell - as a function of magnetic field